

# Supplementary Materials for: Microfluidic Platform for Automatic Quantification of Malaria Parasite Invasion Under Physiological Flow Conditions

Emma Kals<sup>a,b,c,1</sup>, Morten Kals<sup>b</sup>, Viola Introini<sup>a,b,d</sup>, Boyko Vodenicharski<sup>b</sup>, Jurij Kotar<sup>b</sup>, Julian C. Rayner<sup>a,1</sup>, and Pietro Cicuta<sup>b,1</sup>

<sup>a</sup>Cambridge Institute for Medical Research, University of Cambridge, Cambridge, UK

<sup>b</sup>Cavendish Laboratory, University of Cambridge, Cambridge, UK

<sup>c</sup>Center for Cardiovascular Research, University of Edinburgh, Edinburgh, UK

<sup>d</sup>Max-Planck-Zentrum für Physik und Medizin, Erlangen, Germany

<sup>1</sup>Corresponding author

November 30, 2025

## Section S1. Estimation of Hydrodynamic Forces on a Merozoite in the Microfluidic Channel

We estimate the characteristic hydrodynamic forces acting on a  $\sim 1-2 \mu\text{m}$  merozoite as it encounters a red blood cell (RBC) within our microfluidic device. The channel dimensions are  $6 \mu\text{m}$  in height and  $100 \mu\text{m}$  in width, and the suspension (4% hematocrit in culture media) flows at an average velocity of  $U_{\text{avg}} = 410 \mu\text{m s}^{-1}$ . The effective viscosity of the suspension is taken as  $\mu \approx 1.2 \times 10^{-3} \text{ Pa} \cdot \text{s}$ , close to plasma viscosity at low hematocrit.

### Reynolds Number and Flow Regime

Using the channel height  $h = 6 \mu\text{m}$  as the characteristic length, the Reynolds number is

$$\text{Re} = \frac{\rho U_{\text{avg}} h}{\mu} \approx \frac{10^3 \times 4.5 \times 10^{-4} \times 6 \times 10^{-6}}{1.2 \times 10^{-3}} \approx 2 \times 10^{-3} \ll 1.$$

Thus, the flow is well within the creeping flow regime.

### Wall Shear Rate

Because the channel is much wider than it is tall ( $100 \mu\text{m} \gg 6 \mu\text{m}$ ), the flow can be approximated as plane Poiseuille flow between parallel plates. The wall shear rate for such a geometry is

$$\dot{\gamma}_{\text{wall}} \approx \frac{6 U_{\text{avg}}}{h},$$

which yields

$$\dot{\gamma}_{\text{wall}} \approx \frac{6 \times 4.1 \times 10^{-4}}{6 \times 10^{-6}} \approx 410 \text{ s}^{-1}.$$

The corresponding wall shear stress is

$$\tau_{\text{wall}} = \mu \dot{\gamma}_{\text{wall}} \approx (1.2 \times 10^{-3})(410) \approx 0.5 \text{ Pa}.$$

### Hydrodynamic Force Estimates

We model the merozoite as a particle of characteristic size  $L \sim 1 \mu\text{m}$ . Two equivalent Stokes-flow-based approaches give similar force scales.

Table S1: Table showing error rates for each cell type, broken down for each frame and channel.

Strain	Repeat	Experiment	Channel	Time (sec)	Schizonts	Rings	Merozoites	Erythrocytes	Debris
KoRH4 NF54	3	ECK17	0	25.19	0.50	0.00	0.00	0.02	-1.00
KoRH4 NF54	3	ECK17	0	328.75	-	0.00	-0.25	0.02	-1.00
KoRH4 NF54	3	ECK17	1	25.19	0.00	0.00	0.00	0.12	0.00
KoRH4 NF54	3	ECK17	1	328.75	-1.00	-1.00	0.00	0.03	-
KoRH4 NF54	3	ECK17	2	25.19	0.00	-1.00	-	0.17	0.00
KoRH4 NF54	3	ECK17	2	328.75	0.00	0.00	0.00	0.09	0.00
KoRH4 NF54	3	ECK17	3	25.19	0.00	0.00	0.00	0.02	0.00
KoRH4 NF54	3	ECK17	3	328.75	1.00	0.00	0.00	0.03	-0.67
NF54	4	ECK25	0	25.43	2.00	0.00	0.00	0.14	-1.00
NF54	4	ECK25	0	502.37	0.33	-0.30	0.22	-0.04	-0.50
NF54	4	ECK25	1	25.43	0.00	0.00	0.00	0.25	0.00
NF54	4	ECK25	1	502.37	-	-0.08	-0.07	0.10	-1.00
NF54	4	ECK25	2	25.43	-	-	-0.50	0.26	0.00
NF54	4	ECK25	2	502.37	-	-0.12	0.25	0.00	-1.00
NF54	4	ECK25	3	25.43	2.00	0.00	0.00	0.26	-1.00
NF54	4	ECK25	3	502.37	0.00	-0.16	0.07	0.07	0.00
3D7	6	ECK26	0	25.00	0.00	0.00	0.00	0.09	-1.00
3D7	6	ECK26	0	322.69	-	0.40	-0.22	0.19	-1.00
3D7	6	ECK26	1	25.00	-0.29	0.00	-	-0.15	-1.00
3D7	6	ECK26	1	322.69	0.00	0.25	0.00	0.11	0.00
3D7	6	ECK26	2	25.00	-	0.00	0.00	0.26	0.00
3D7	6	ECK26	2	322.69	-	0.09	0.11	0.28	-1.00
3D7	6	ECK26	3	25.00	-	0.00	-1.00	0.38	-1.00
3D7	6	ECK26	3	322.69	0.00	0.22	-0.11	0.40	0.00
NF54	5	ECK27	0	51.00	0.00	0.00	-0.50	0.18	-1.00
NF54	5	ECK27	0	486.26	0.00	-0.33	0.25	0.36	0.00
NF54	5	ECK27	1	51.00	1.00	0.00	0.00	0.27	-1.00
NF54	5	ECK27	1	486.26	0.00	-0.47	0.14	0.25	0.00
NF54	5	ECK27	2	51.00	2.00	0.00	0.00	0.49	-1.00
NF54	5	ECK27	2	486.26	-	-0.41	0.14	0.15	0.00
NF54	5	ECK27	3	51.00	0.00	-1.00	-	-0.03	0.00
NF54	5	ECK27	3	486.26	-	-0.31	0.25	0.28	-

**(1) Shear Stress Acting over the Particle Area** Taking the exposed area as surface area of a sphere  $A = \pi d^2 \approx 1.2 \times 10^{-11} \text{ m}^2$ ,

$$F \approx \tau_{\text{wall}} A = 6.2 \times 10^{-12} \text{ N} \approx 6 \text{ pN}$$

**(2) Stokes Drag in a Linear Shear Field** Near the wall, the velocity profile is approximately linear, giving a relative velocity  $U_{\text{rel}} \sim \dot{\gamma}_{\text{wall}} L$ . The Stokes drag on a sphere of radius  $a \approx 1 \mu\text{m}$  in such a flow is

$$F \approx 6\pi\mu a U_{\text{rel}} = 6\pi\mu a^2 \dot{\gamma}_{\text{wall}}.$$

Substituting values,

$$F \approx 6\pi(1.2 \times 10^{-3})(10^{-6})^2(410) \approx 9.3 \times 10^{-12} \text{ N} \approx 10 \text{ pN}.$$

## Resulting Force Scale

Both methods produce consistent estimates around 10 pN.

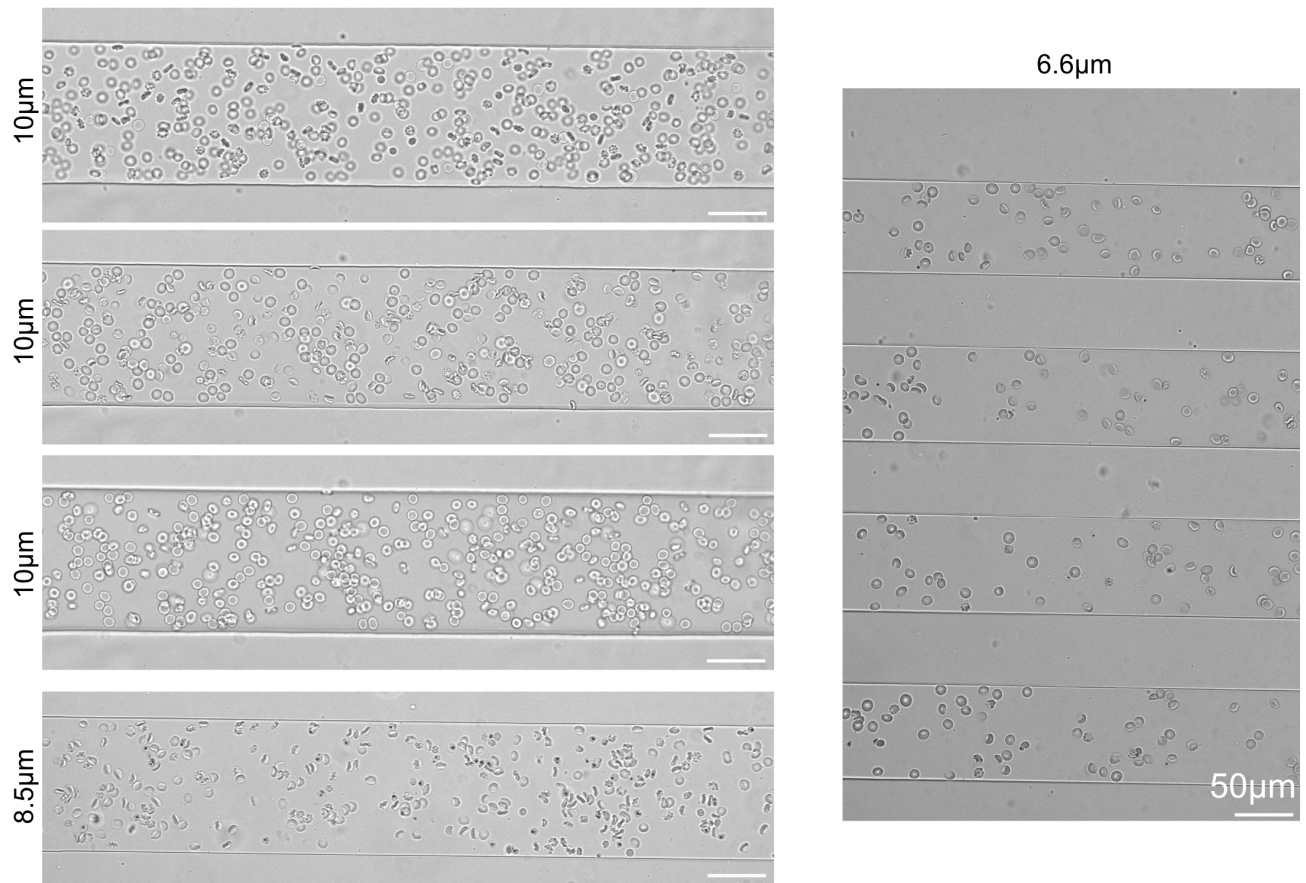


Figure S1: **Examples of parasites imaged in channels of different depths.** Three images are shown for the 10  $\mu\text{m}$  channel at three different depths of focus. The 8.5  $\mu\text{m}$  and 6.6  $\mu\text{m}$  channels are shown at a single focus. Error bars are 50  $\mu\text{m}$ . The 10  $\mu\text{m}$  and 8.5  $\mu\text{m}$  deep channels show erythrocytes in the single-channel device with a 100  $\mu\text{m}$  width. The 6.6  $\mu\text{m}$

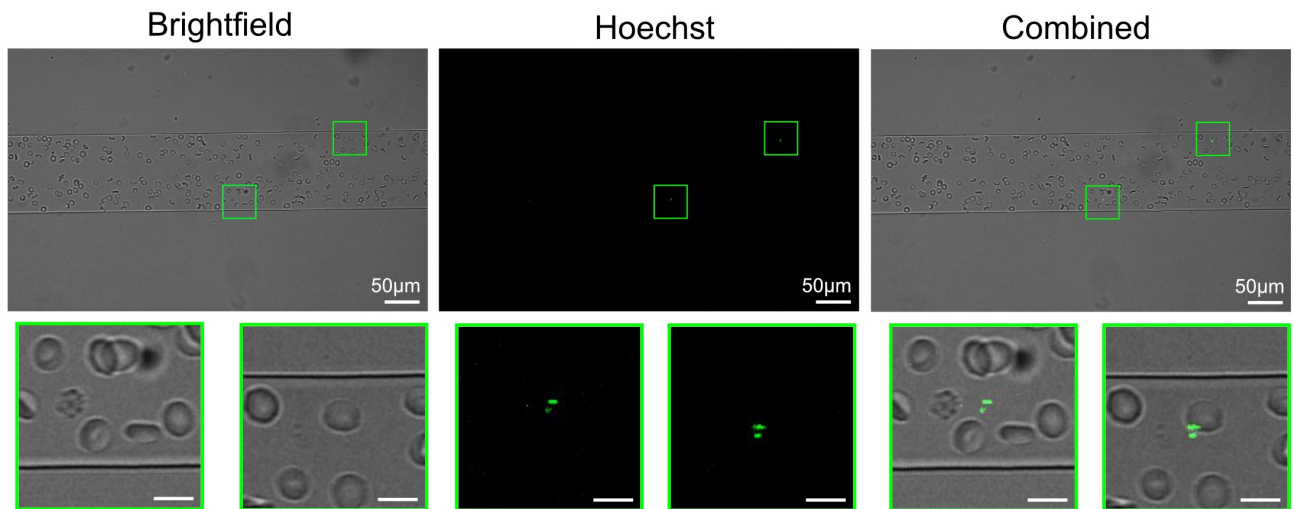


Figure S2: **Comparison of infected erythrocytes in a microfluidics channel under flow with Hoechst 33342** Unless indicated otherwise, the scale bars are 10  $\mu\text{m}$ . Images were taken with a 20x objective. Infected erythrocytes stained with Hoechst 33342 at 1 in 10000 concentration for 10 mins. The experiment was run with a single channel device with a 100  $\mu\text{m}$  width and 10  $\mu\text{m}$  depth. The green boxes contain at least one example of a ring (when the erythrocytes are followed across the channel, the fluorescent signal stays with them).

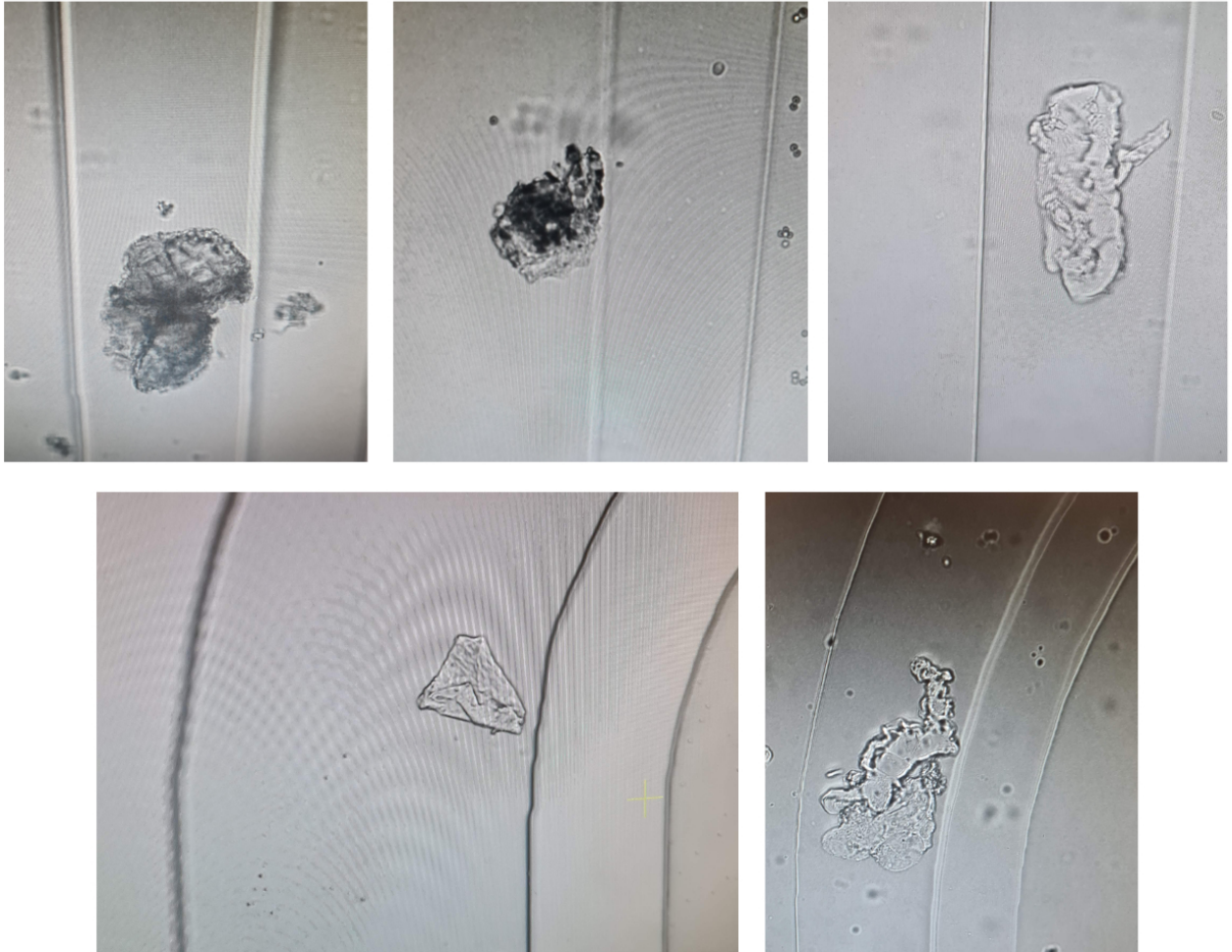


Figure S3: **Examples of non-cell debris seen in microfluidics channels.**

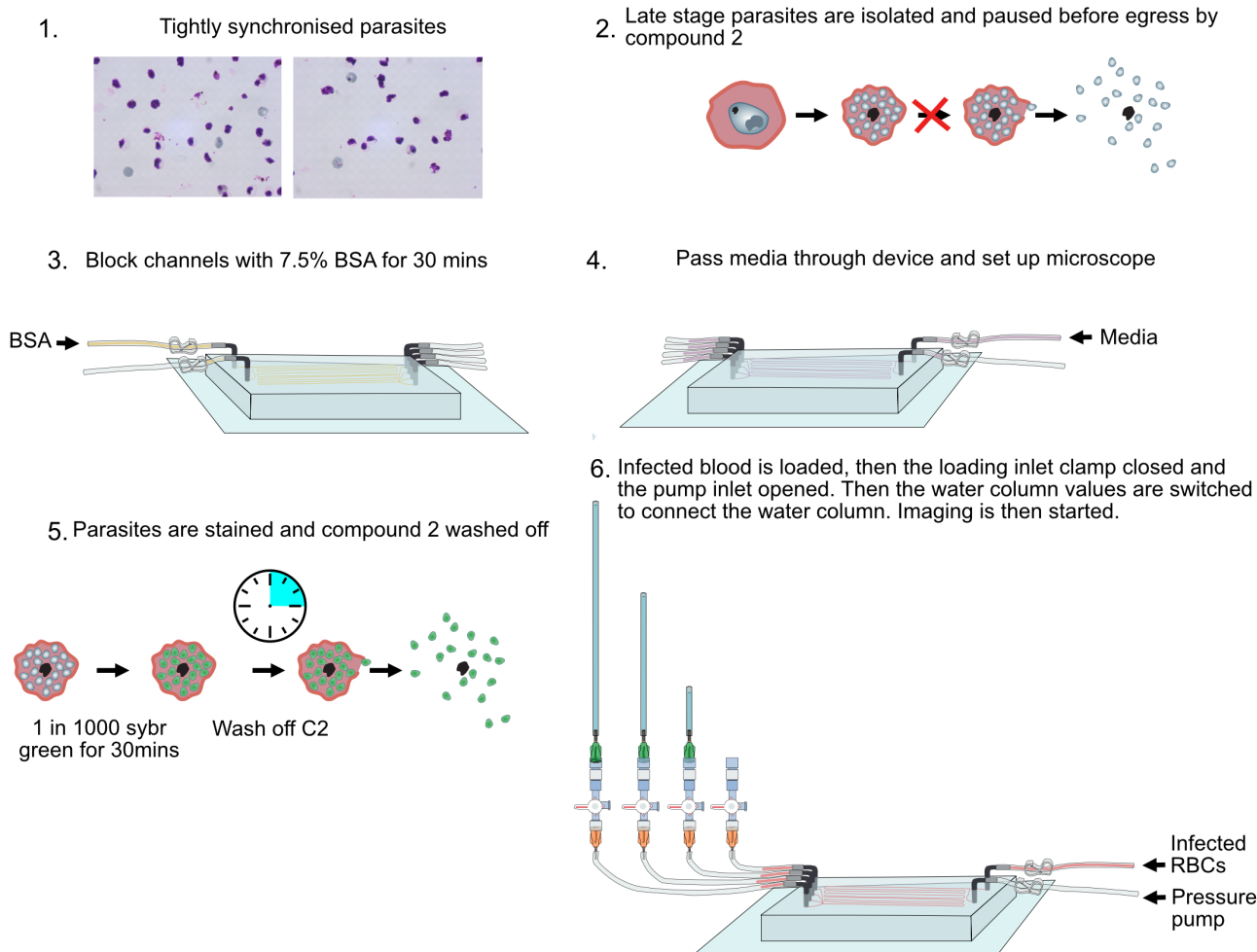


Figure S4: **Summary of microfluidic experiment workflow** On the day of the experiment, Schizonts are isolated from a sample which has been tightly synchronised to the correct time window using Percol. These are then resuspended in compound 2 for 3-5.5 hours. The microfluidics chip is set up, and 7.5% BSA is passed into the channel and left for 30 mins at 37°C. An aliquot of the sample is then pelleted and resuspended in sybr green and Compound 2 for 30 mins. The chip is then transferred to the microscope and connected to the inlet, outlet and pump tubes. The pump is turned on but the tube to it is clamped. Media is passed through the chip to confirm that there are no leaks; if any sign of detachment is detected, the chip is discarded. The chip is aligned, and the microscope focuses on the imaging field of view, ensuring that all channels are in focus. The Compound 2 is then washed off the parasite sample, blood is added to give the desired hematocrit and it is loaded into a syringe. This then gives a 10 min time window to load the sample into the chip via the inlet. The sample is loaded until it is seen in all the channels and ideally in the outlet tubing. The inlet is then clamped, the pump inlet tubing unclamped and then the valves to the water columns switched so the column is connected to the outlet.

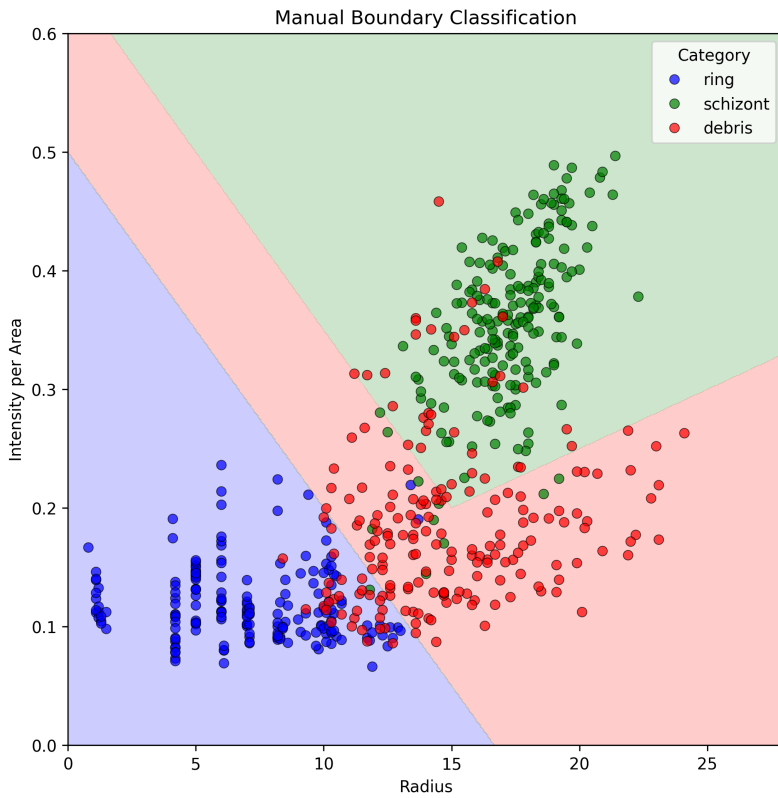


Figure S5:

Graph to show how rings/merozoites, schizonts and debris were distinguished. Frames containing a cropped section of the brightfield and fluorescent image of different cells were exported from several videos. They were then manually classified as rings/merozoites, schizonts or debris. The intensity per area vs the radius of the fluorescent signal from the SYBR Green DNA dye for each cell was plotted. Boundaries were then defined between the three groups to maximise the correct classification of the three cell types. This is possible because rings/merozoites have a single copy of the genome, resulting in a small radius and a low-intensity signal. Schizonts have multiple copies of the genome tightly packed together, resulting in a fluorescent signal which is both larger in radius and more intense. Debris is likely made up of fragments of the infected RBC, stuck merozoites and/or hemozoin crystals. The radius and intensity of debris there tends to be between that of the rings/merozoites and schizonts.

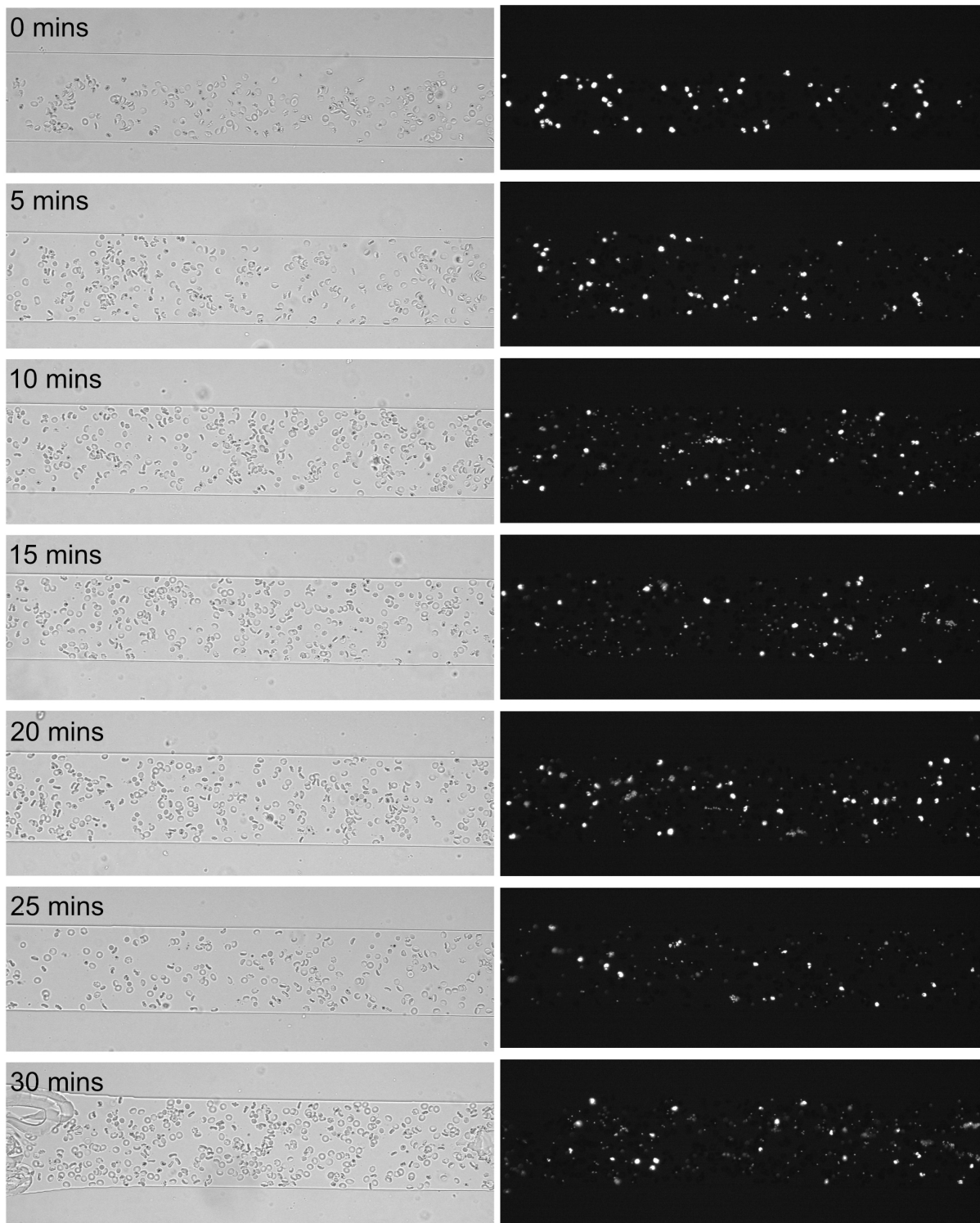
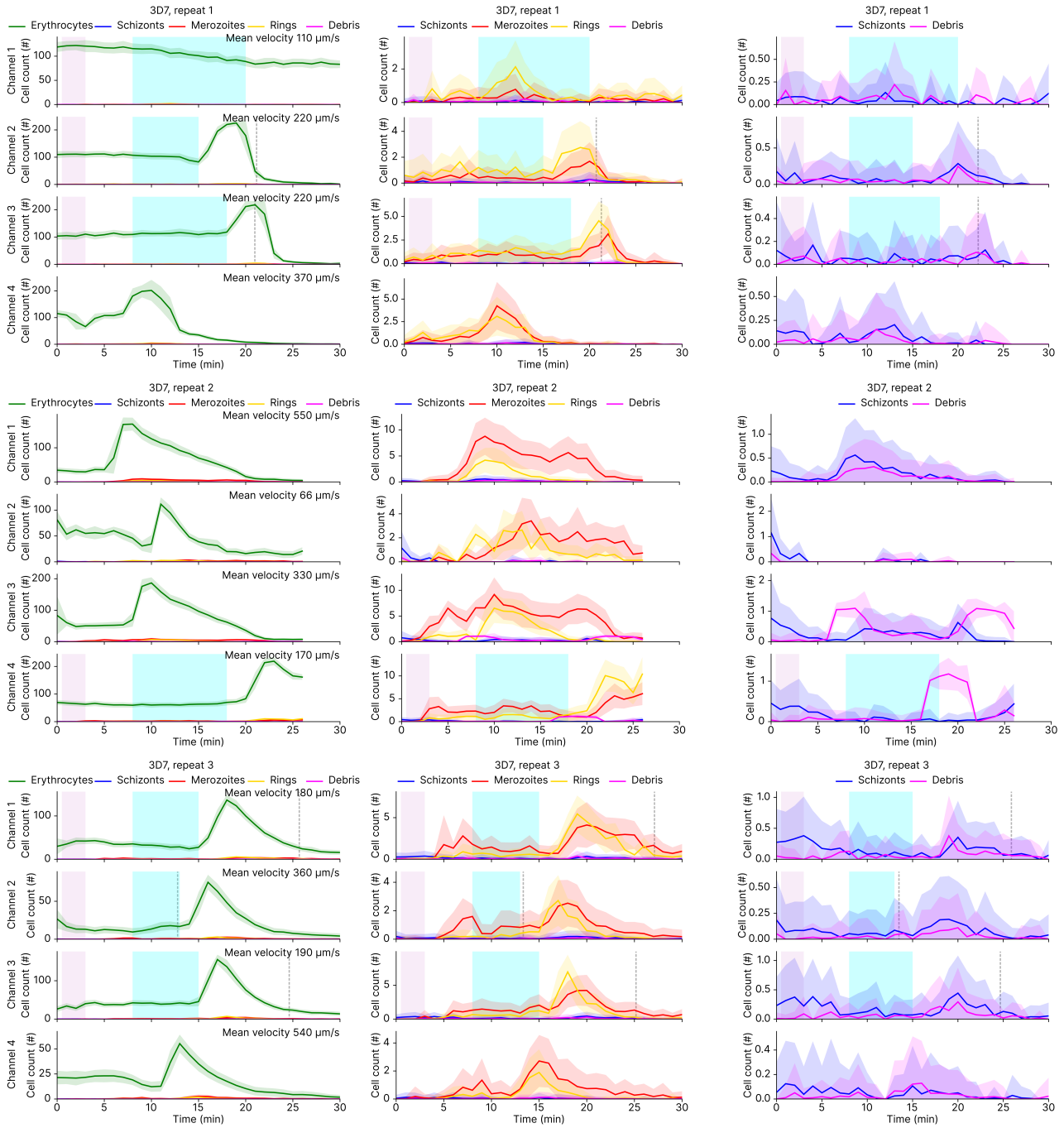
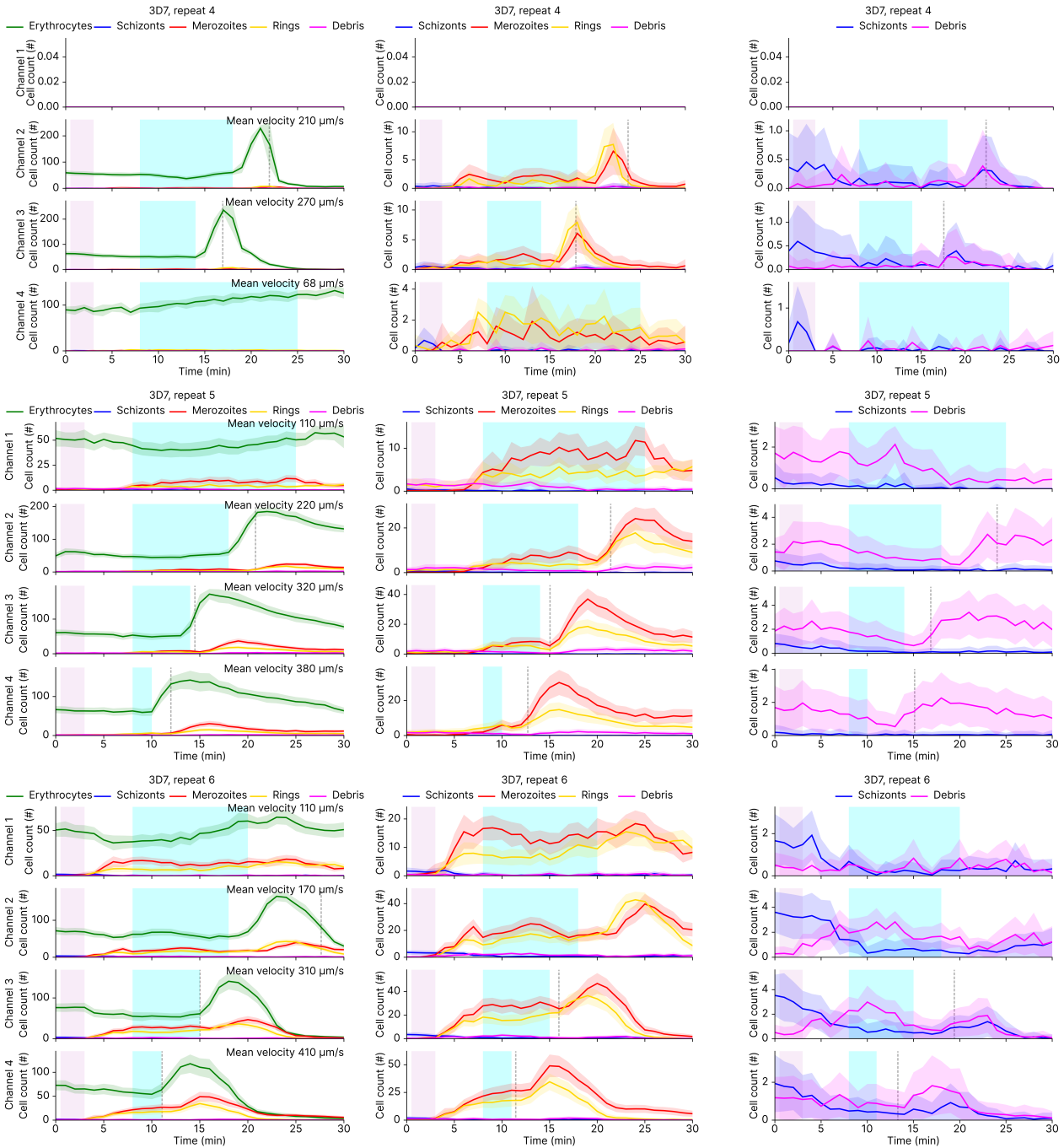


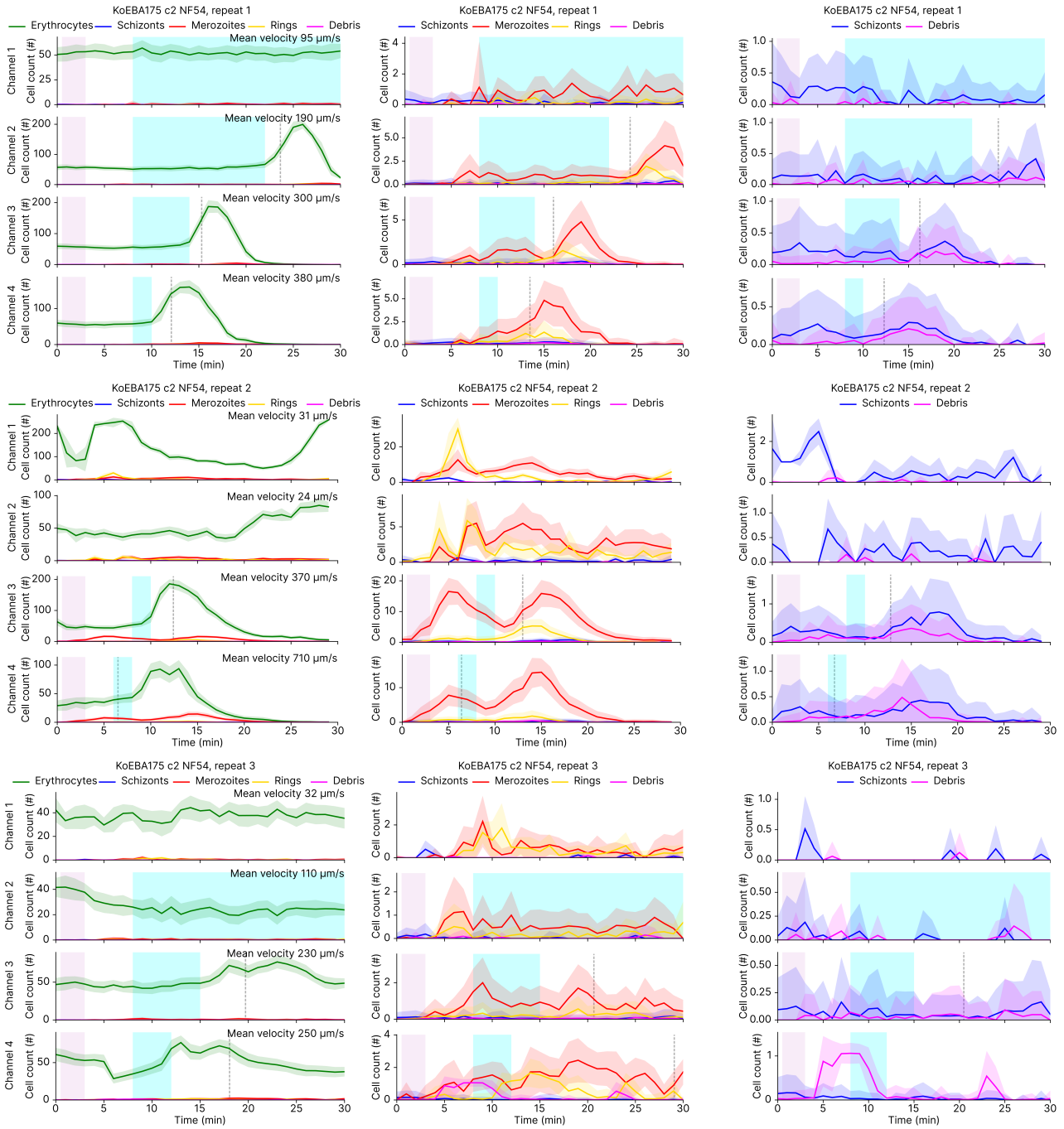
Figure S6: **Example of frames taking over the course of an experiment to show the visual change in the proportion of different cell types.** Infected erythrocytes were stained with Sybr Green at a 1 in 5000 concentration for 45 mins. Time 0 is the time at which imaging began for this sample. Examples are shown of brightfield and fluorescent frames taken every 5 mins of the experimental run. The position of imaging was changed every 5 mins; the positions were determined based on the approximate flow rate of the cells so that roughly the same cells were imaged in every 5 mins segment. The experiment was run with a single channel device with a 100  $\mu\text{m}$  width and 8.5  $\mu\text{m}$  depth. The early images have a higher density of schizonts, then as time goes on, more merozoites are released as the schizonts egress. In the final image, there is a lower density of schizonts but a much higher density of small foci that indicate merozoite/rings.



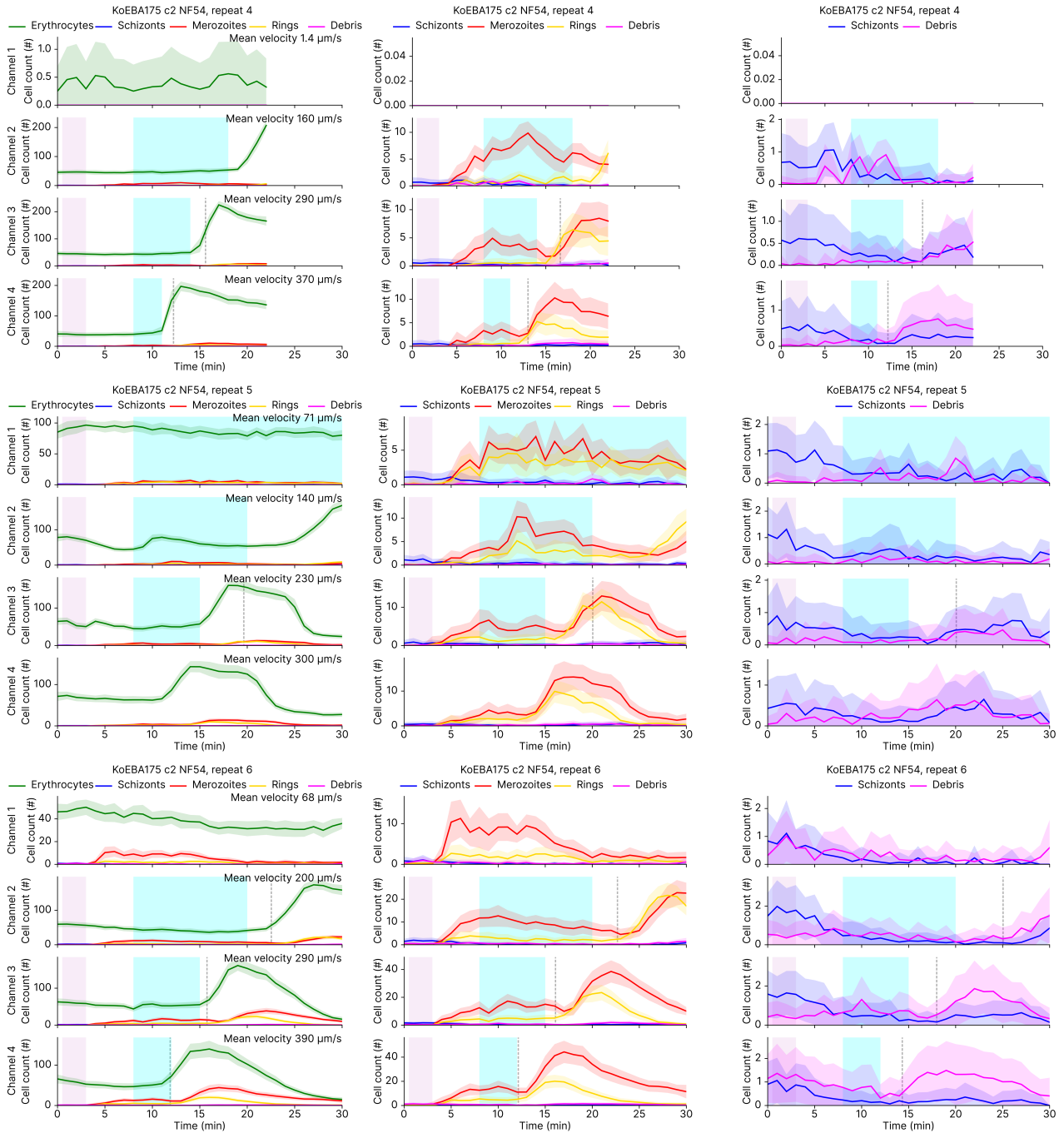
(a)



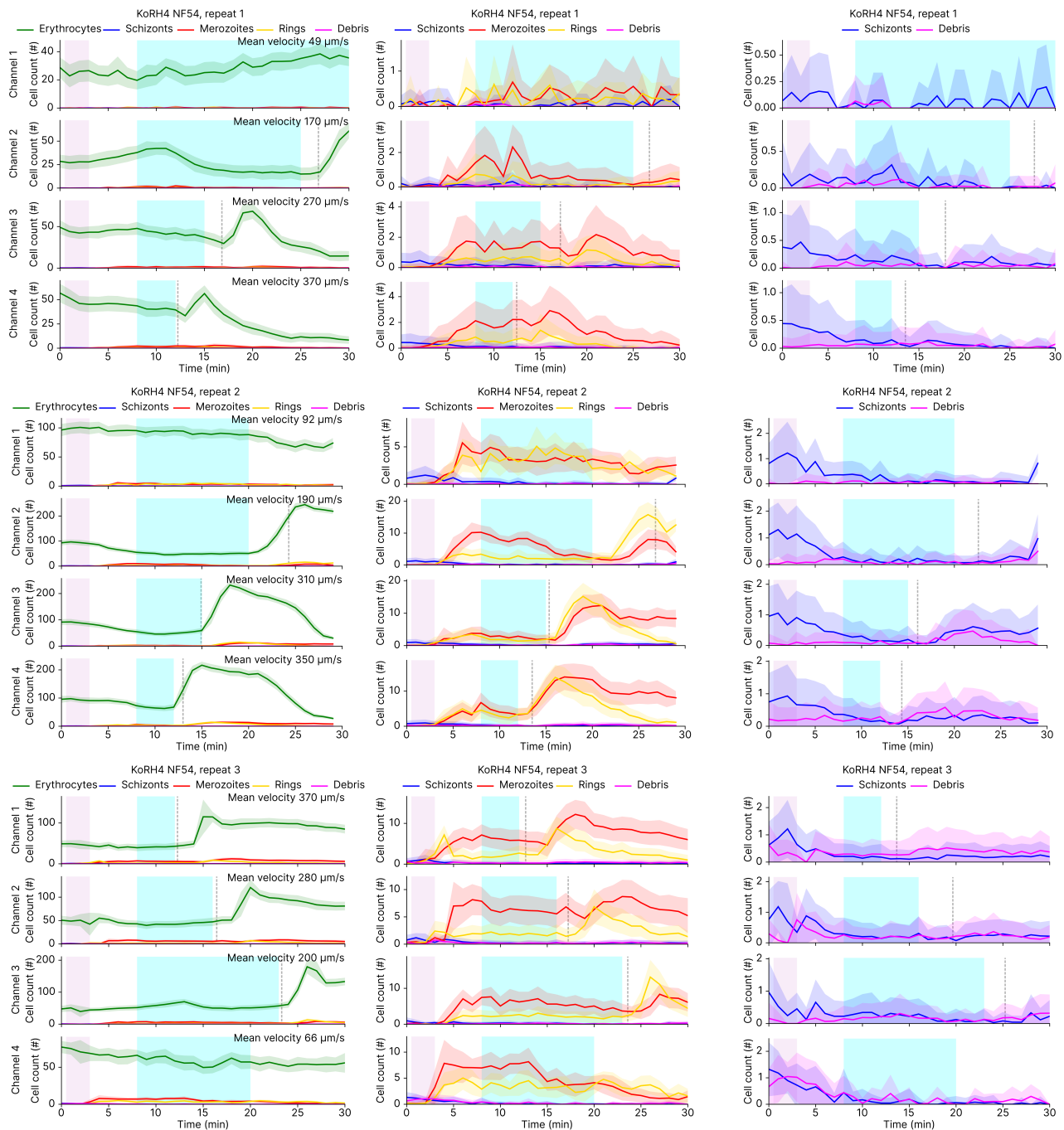
(S7.b)



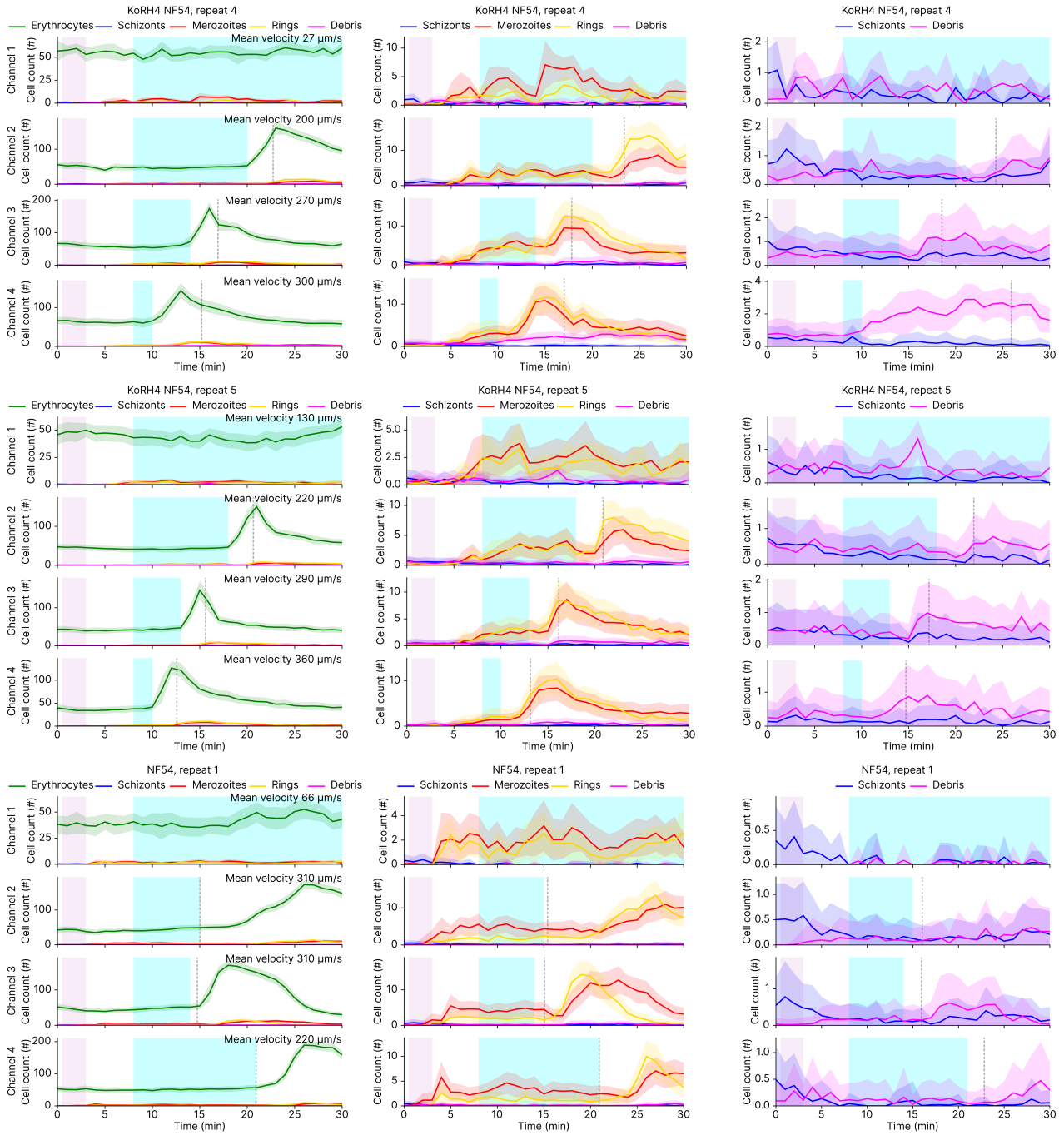
(S7.c)



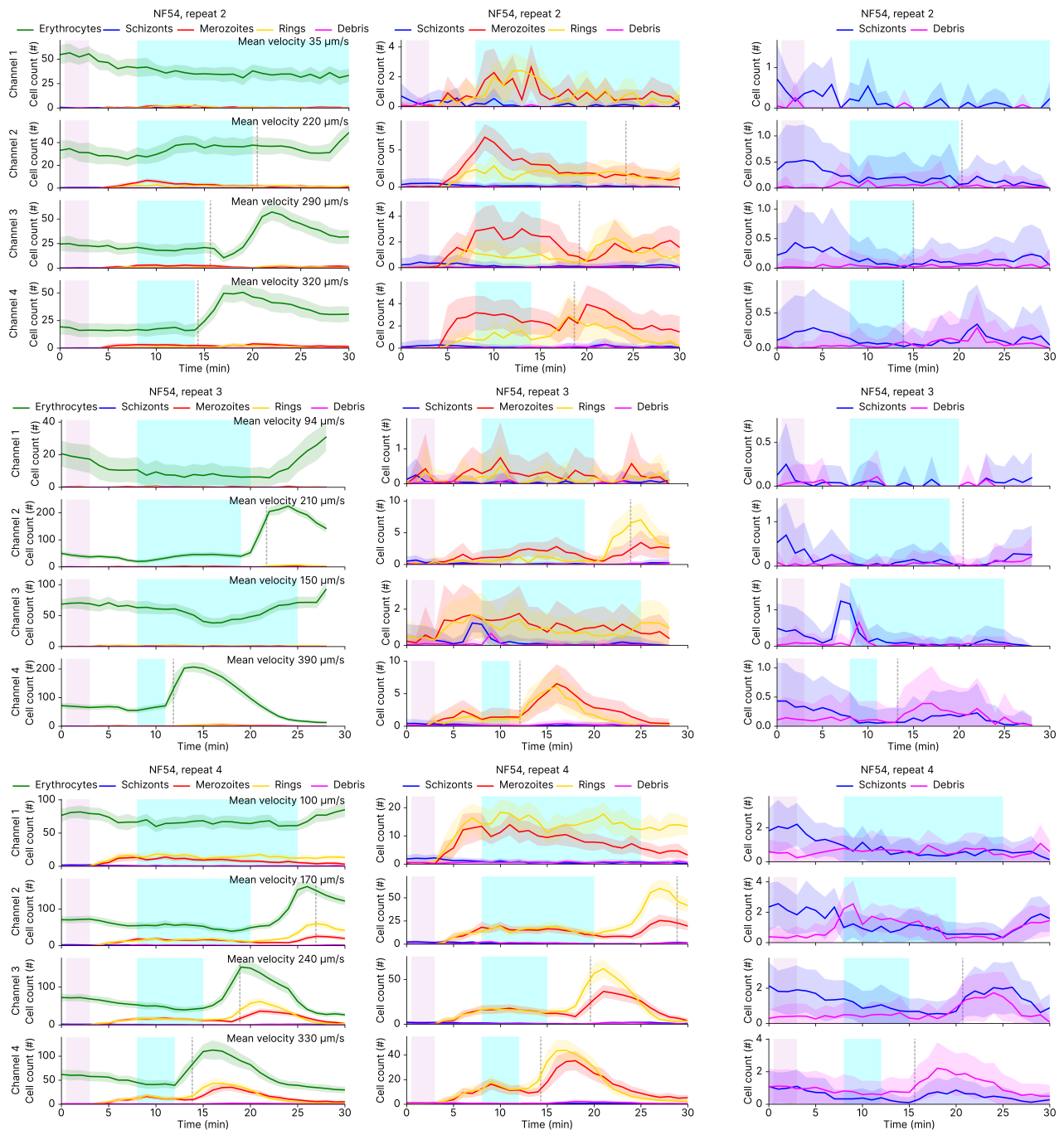
(S7.d)



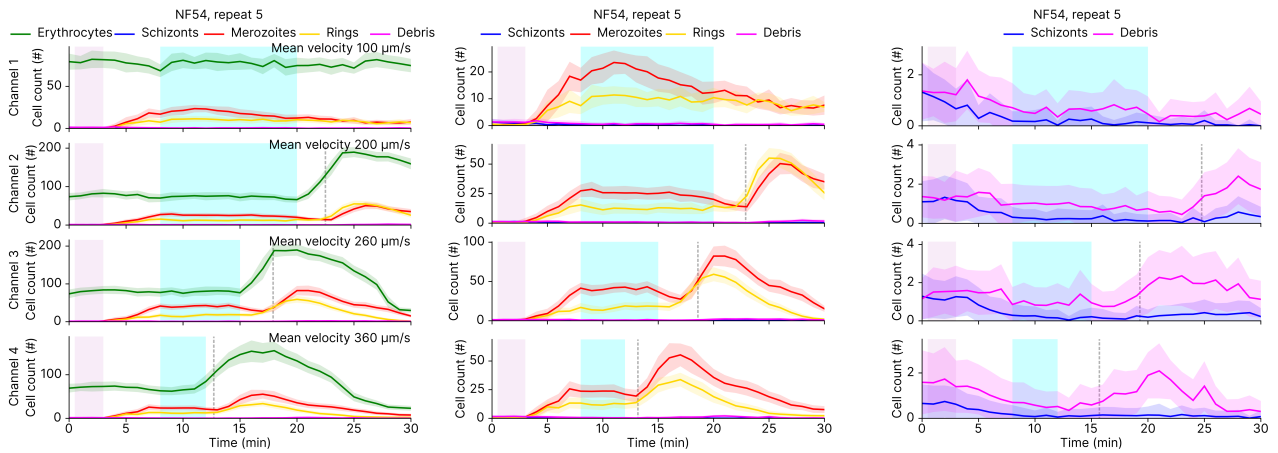
(S7.e)



(S7.f)

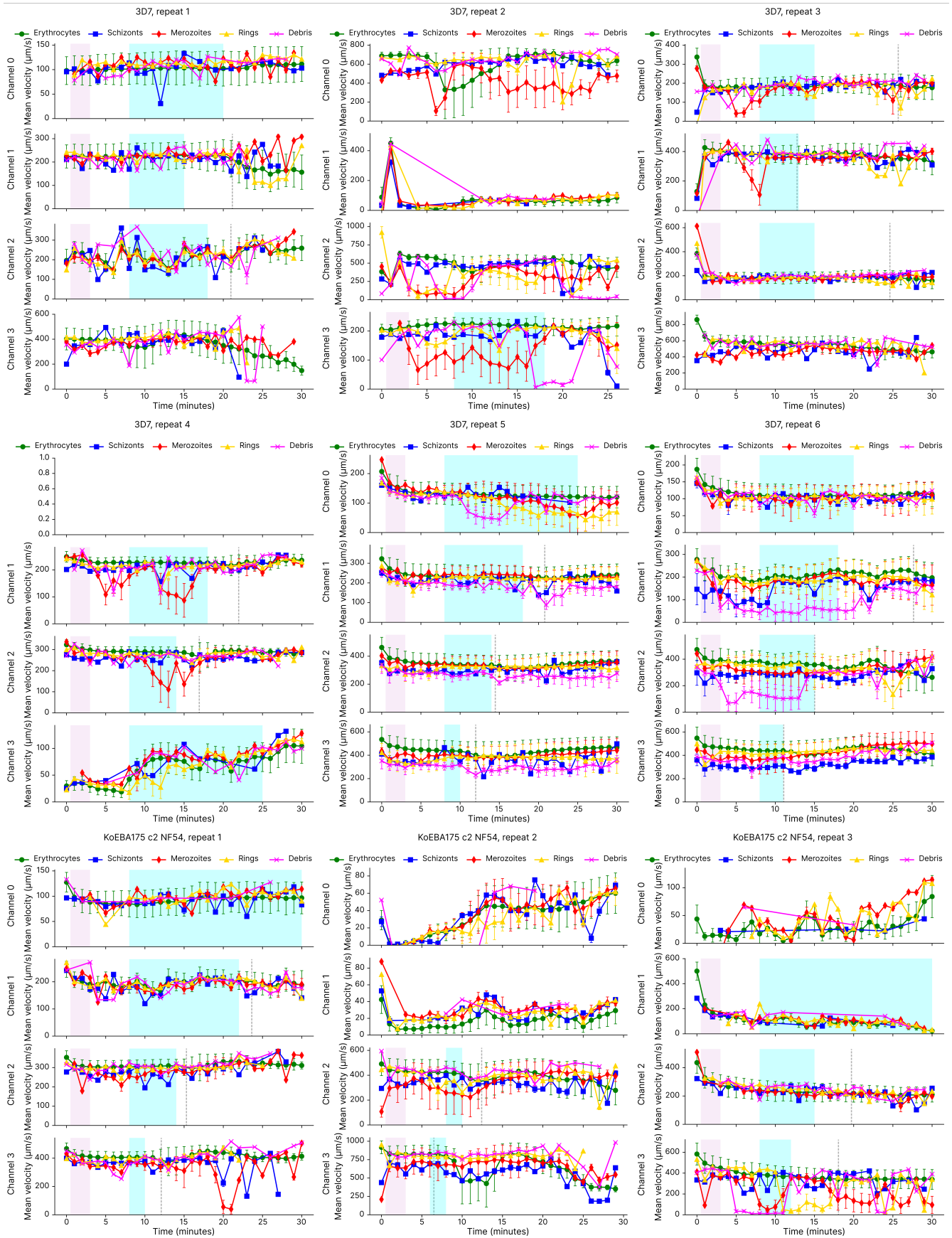


(S7.g)

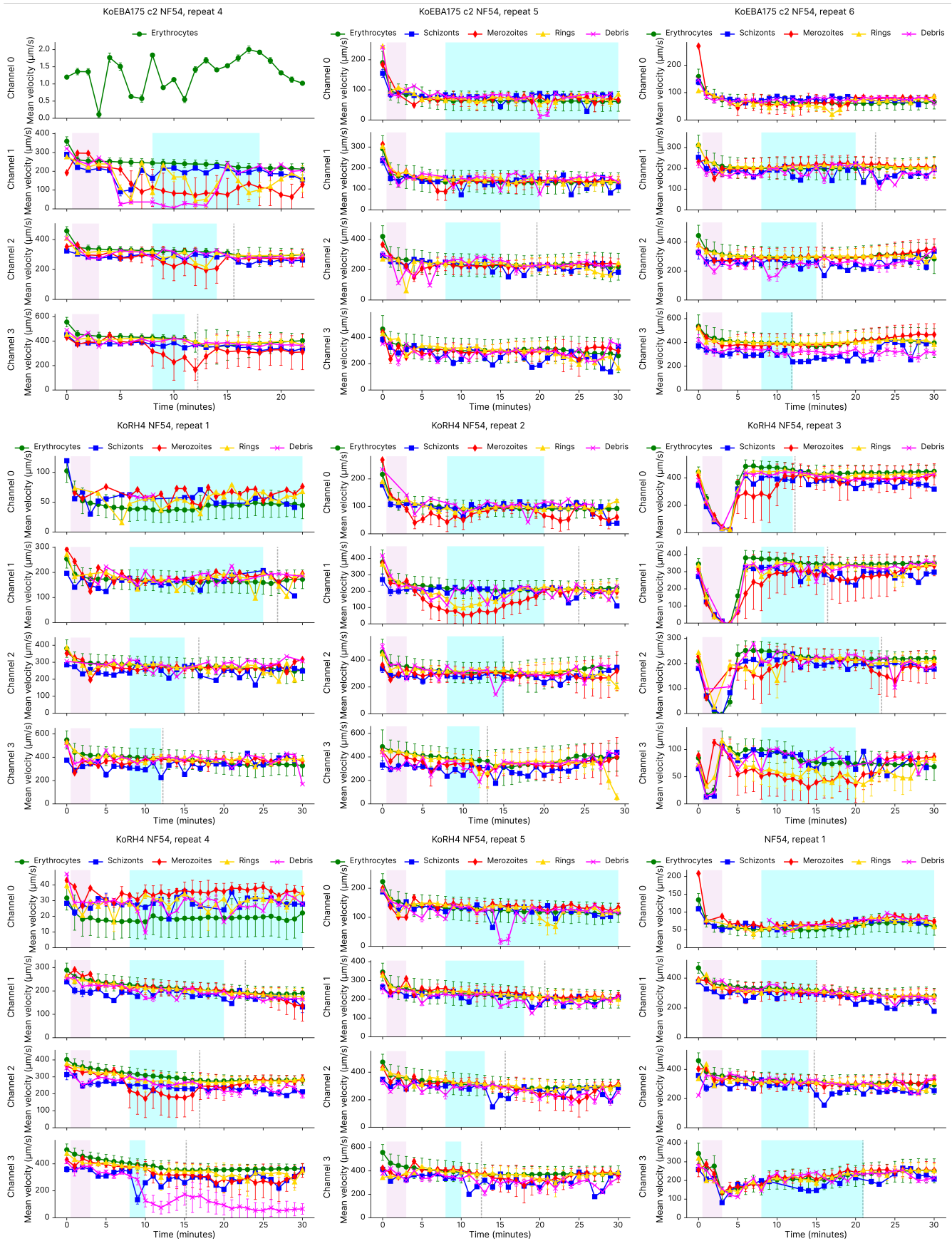


(h)

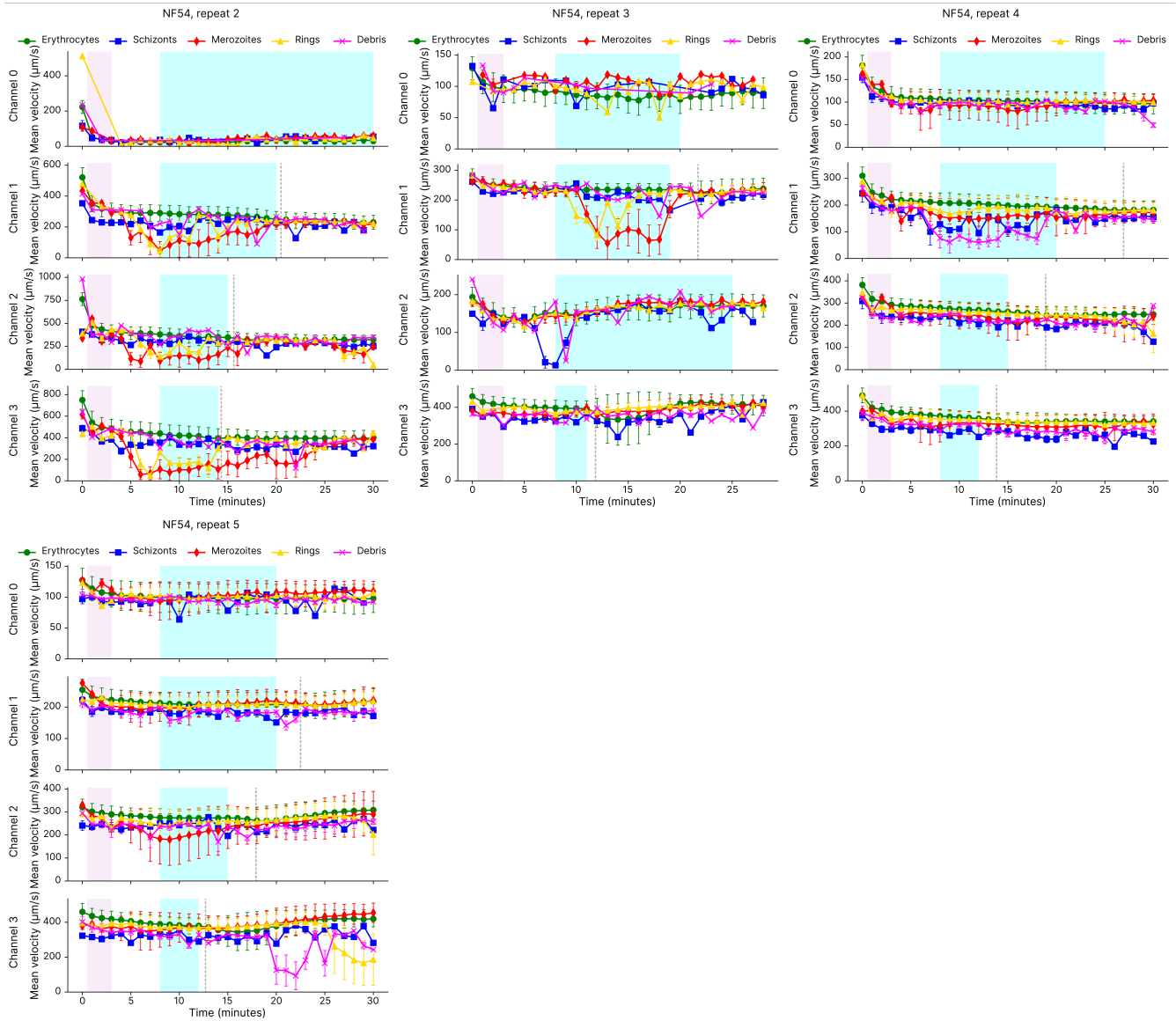
Figure S7: **Changes in cell counts of different cell types over time.** Plots show the change in different cell types' count over time for each experiment run. There are three plots for each experiment, each showing a different scale, so that the different cell types are clear.



(a)

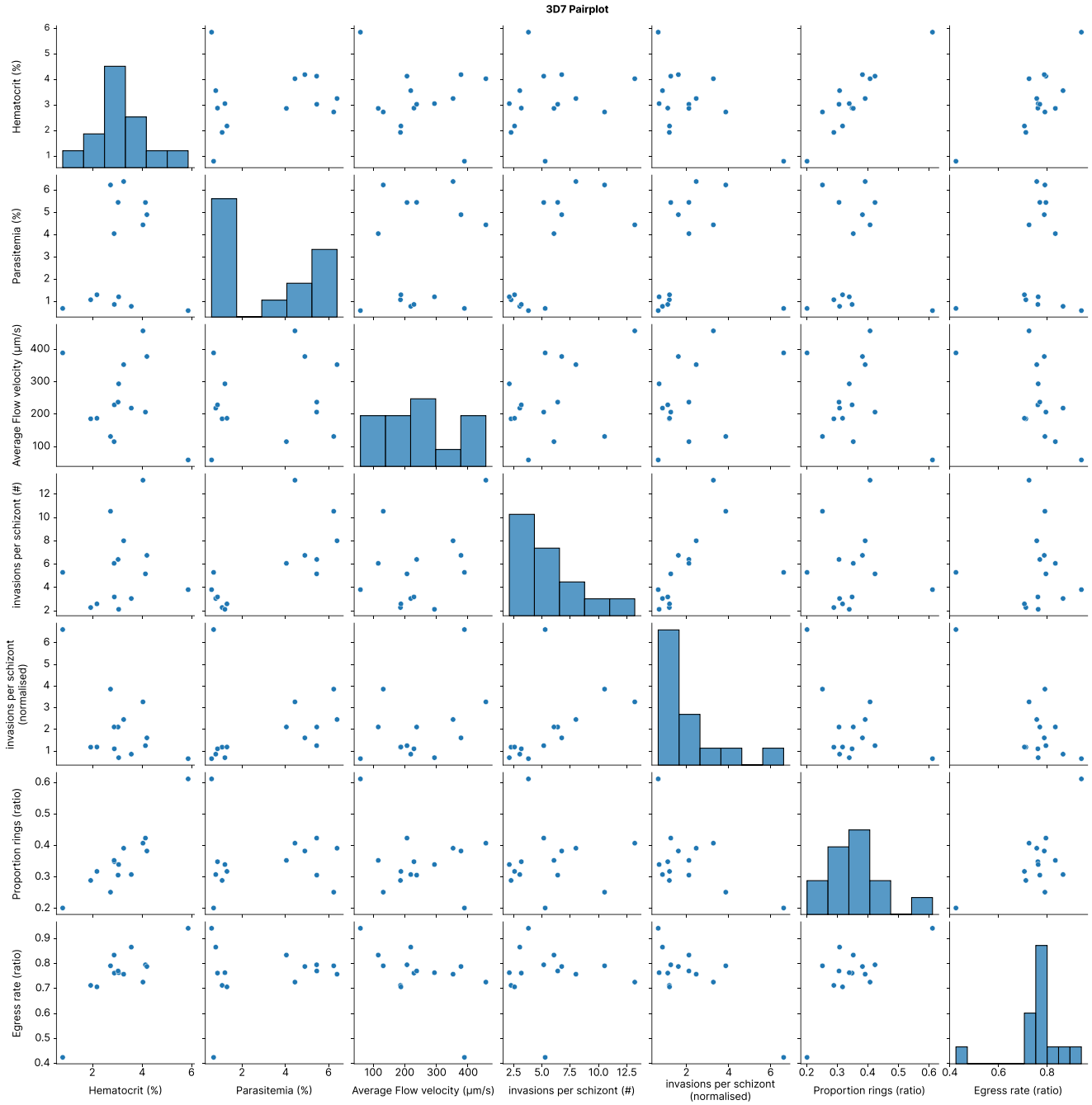


(S8.b)

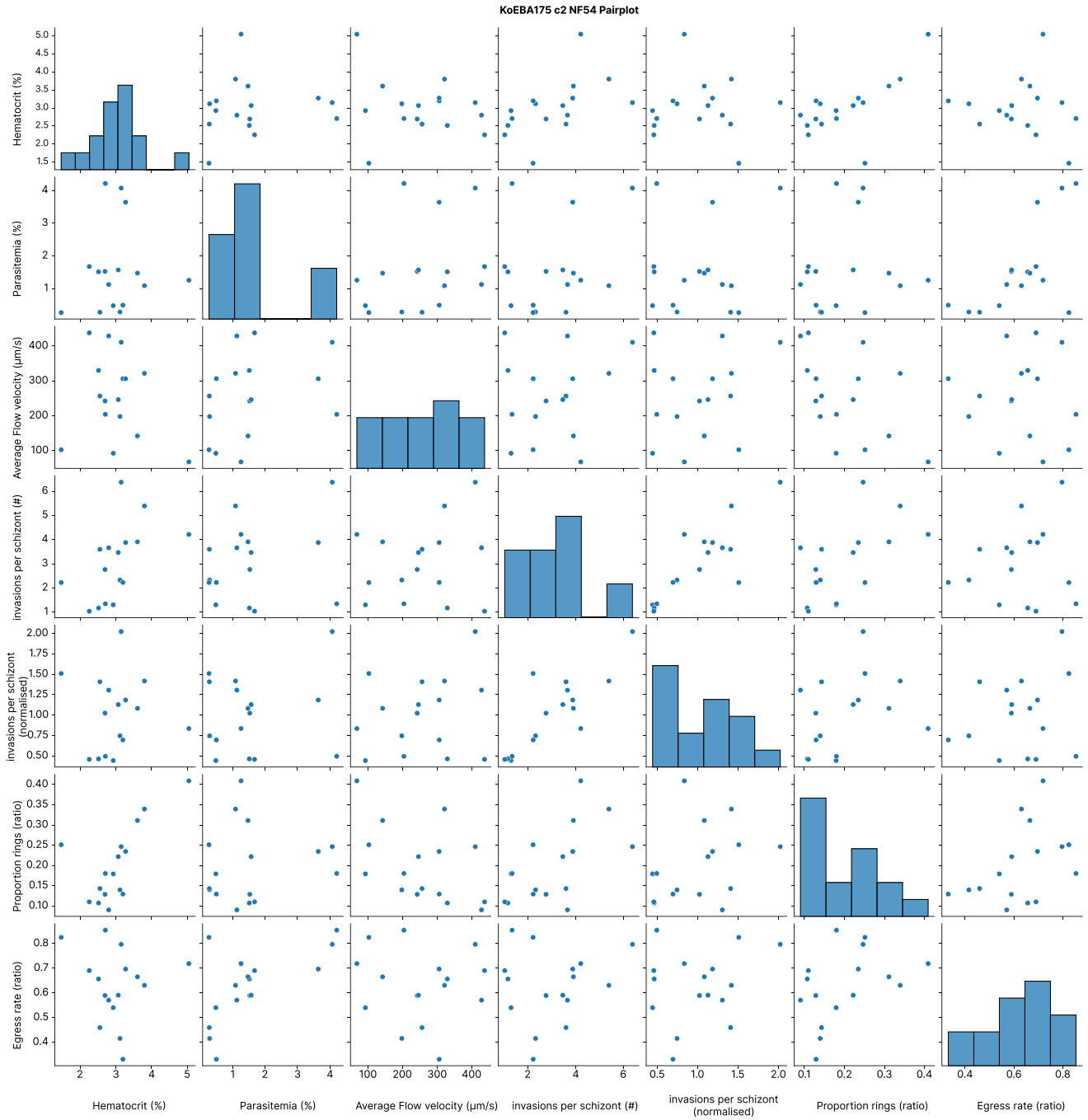


(c)

Figure S8: Changes in flow rate of different cell types over time.

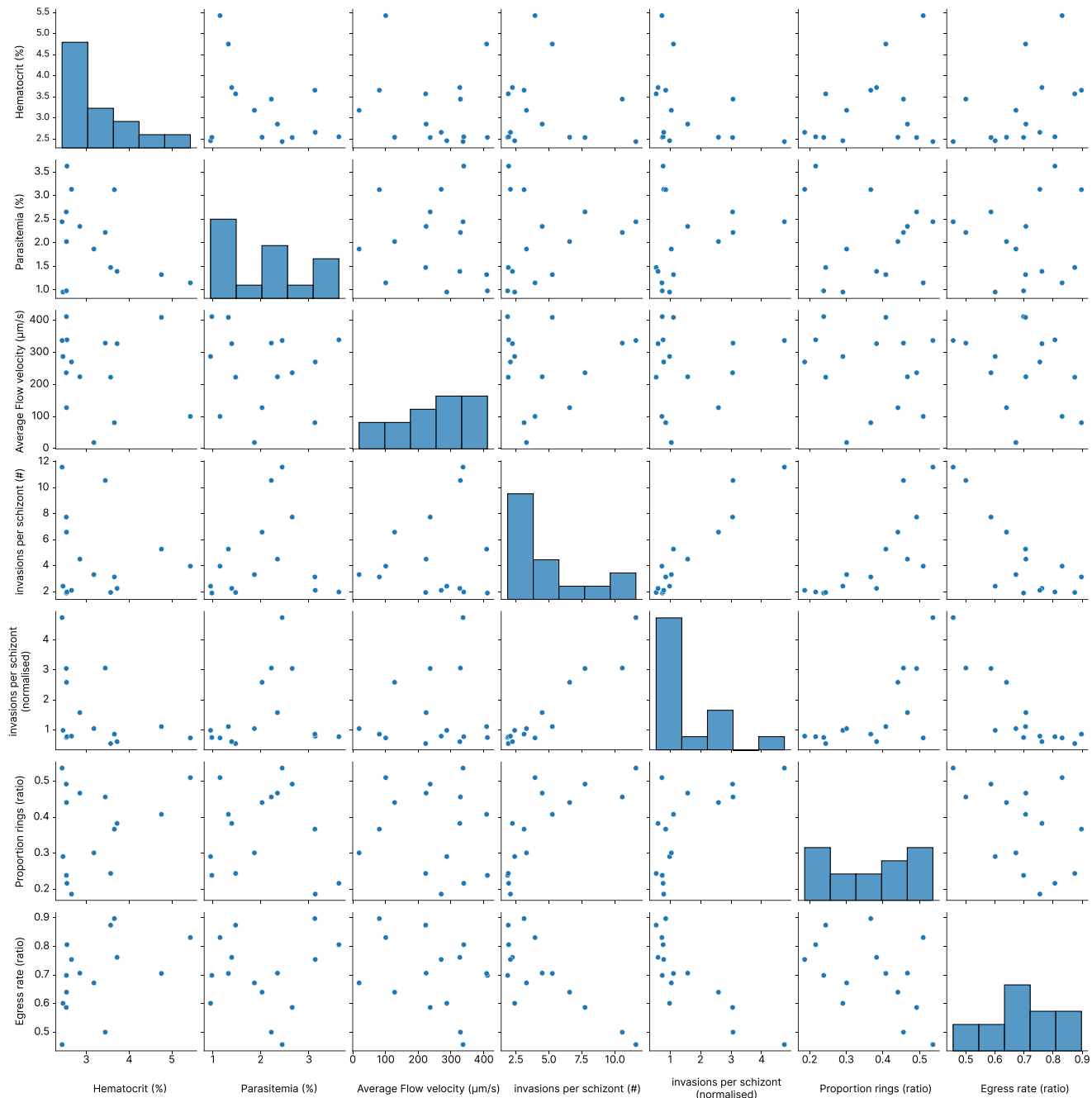


(a)

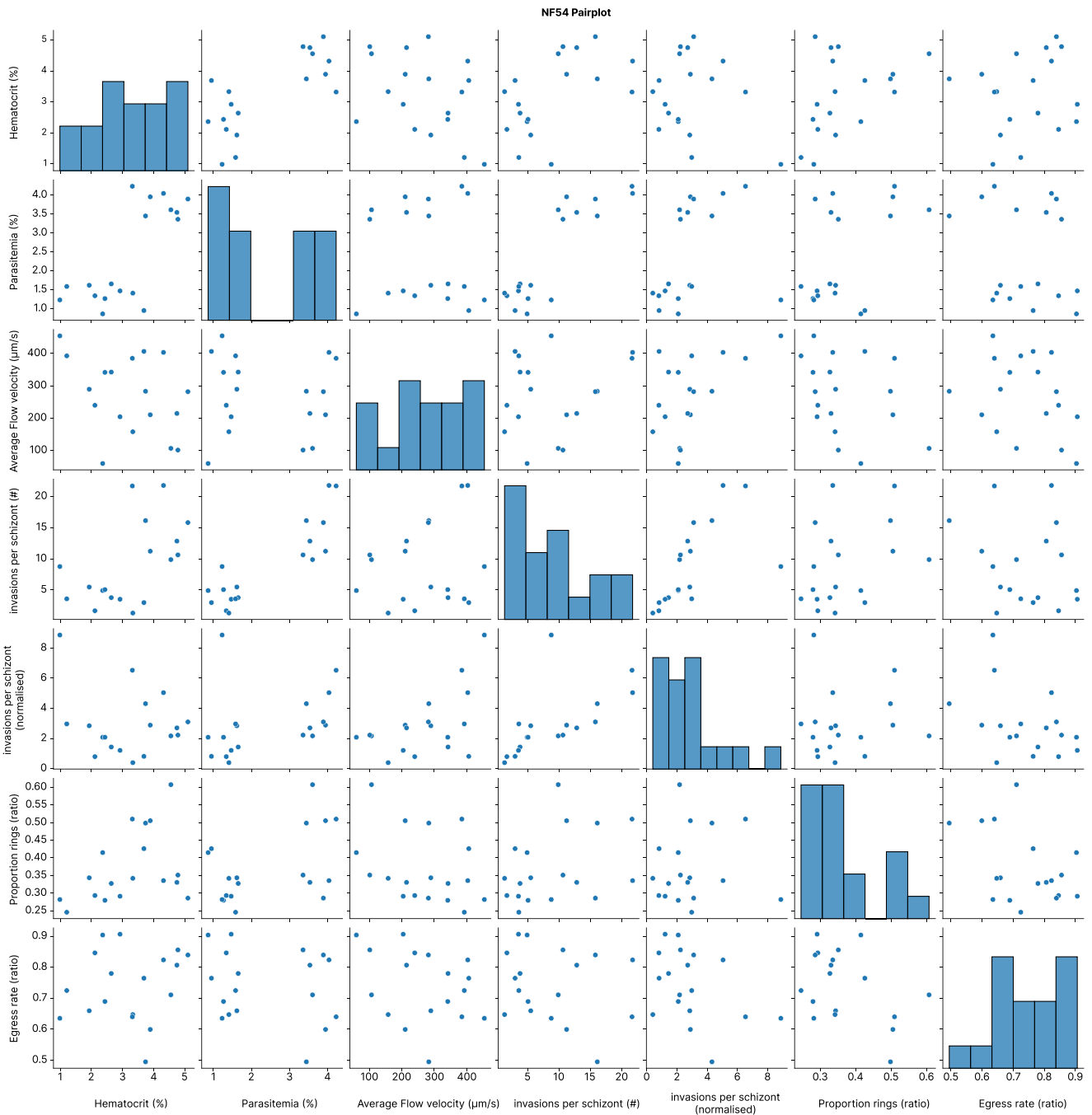


(S9.b)

KoRH4 NF54 Pairplot



(S9.c)



(d)

Figure S9: **Pairplots showing all combinations of variables considered for each species in turn.** Each point represents data from one channel and repeat.

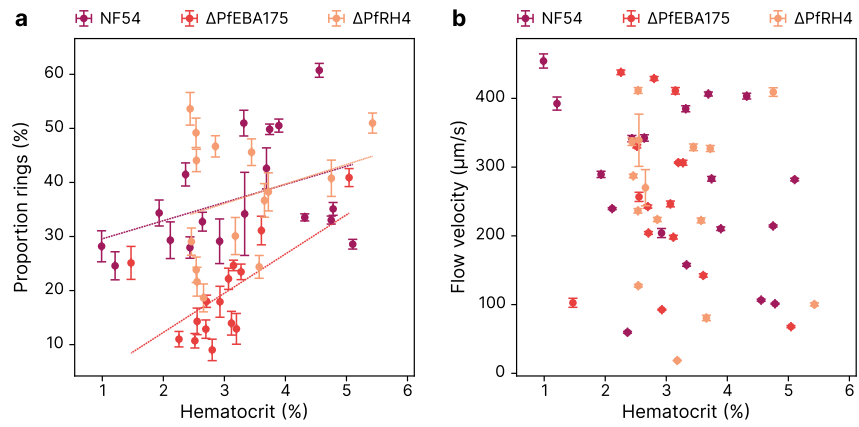


Figure S10: Showing relationship between hematocrit, proportion rings and flow velocity for EBA175 and the two corresponding knock-out lines  $\Delta$ PfEBA175 and  $\Delta$ PfRH4. Each point represents data from one channel during one repeat of the experiment. Both A and B have error-bars in x and y representing standard deviation.